CZECH POLAR REPORTS 12 (1): 131-142, 2022

Multispectral aerial monitoring of a patchy vegetation oasis composed of different vegetation classes. UAV-based study exploiting spectral reflectance indices

Peter Váczi*, Miloš Barták

Laboratory of Photosynthetic Processes, Department of Experimental Biology, Faculty of Science, Masaryk University, Kamenice 5, 625 00 Brno, Czech Republic

Abstract

The study brings data on monitoring of spectral refectance signatures of different components of Antarctic terrestrial vegetation by using a high-resolution multispectral images. The aim of the study was to compare several spots of a vegetation oasis by mapping vegetation cover using an UAV approach. This study provides data on vegetation distribution within a long-term research plot (LTRP) located at the northern coast of James Ross Island (Antarctica). Apart from normalized difference vegetation index (NDVI), 10 spectral reflectance indices (NDVI, $NDVI_{Red\text{-}edge}$, RGBVI, NGRDI, ExG, TGI MSR, $MSR_{Red\text{-}edge}$, Cl_{green}, $Cl_{Red\text{-}edge}$, GLI) were evaluated for different spots representing vegetation classes dominated by different Antarctic autotrophs. The UAV application and spectral reflectance indices proved their capability to detect and map small-area vegetated patches (with the smallest area of 10 cm^2) dominated by different Antarctic autotrophs, and identify their classes (moss / lichens / biological soil crusts / microbiological mats / stream bottom microbiological mats). The methods used in our study revealed sufficiently high resolution of particular vegetation-covered surfaces and the spectral indices provided important indicators for environmental characteristics of the long-term research plot at the James Ross Island, Antarctica.

Key words: remote sensing, UAV, James Ross Island, vegetation mapping, spectral reflectance, functional substrate types

DOI: 10.5817/CPR2022-1-10

Symbols and abbreviations: LTRP – long-term research plot (on James Ross Island), NDVI - normalized difference vegetation index, R – red, G – green, B – blue, NGRDI – Normalized Green-Red Difference Index, GLI – Green Leaf Index, TGI – Triangular Greenness Index, RGBVI – Red-Green-Blue Vegetation Index, ExG – Normalized Excess Green Index, $NDVI_{Red\text{-}edge}$ – Red-edge Normalized Difference Vegetation Index, MSR – Modified Simple Ratio Index, $MSR_{Red\text{-}edge}$ – Red-edge Modified Simple Ratio Index, CI_{green} – Green Chlorophyll Index, $Cl_{Red\text{-}edge}$ – Red-edge Green Chlorophyll Index

---

Received April 18, 2022, *accepted* August 30, 2022.
*Corresponding author: P. Váczi <vaczi@sci.muni.cz>
Acknowledgements: The study reported in this paper was supported by the ECOPOLARIS project (CZ.02.1.01/0.0/0.0/ 16_013/0001708) provided by the Czech Ministry of Education, Youth, and Sports. The authors are grateful to the CzechPolar2 (LM2015078) for the possibility to use laboratory infrastructure. Computational resources were supplied by the project "e-Infrastruktura CZ" (e-INFRA LM2018140) provided within the program Projects of Large Research, Development and Innovations Infrastructures.

Introduction

Remote sensing is considered a very efficient tool for mapping and monitoring of Arctic (Beamish et al. 2020) and Antarctic (for review *see* Pina and Vieira 2022) terrestrial ecosystems. In the last decade, unmanned aerial vehicles (UAV) carrying spectral cameras have been used more and more to identify component of vegetation cover in polar regions (Fraser et al. 2016, Jawak et al. 2019, Siewert and Olofsson 2020). In Antarctica UAVs are used for characterization of vegetation oases and general vegetation mapping. Moreover, other types of vegetation cover, such as, *e.g.* microbiological mats (Levy et al. 2020), and snow algae (Gray et al. 2020) are distinguished by UAV as well. The cameras used are either visible or narrow-band multispectral ones (*see* e.g., Lucieer et al. 2014, Turner et al. 2014).

Within last decades, vegetation classes have been typically distinguished in remote sensing studies focusing to vascular plants in subpolar regions (Eischeid et al. 2021). In Antarctic vegetation, however, classification of particular vegetation components (typically non-vascular autotrophs) is reported just recently (Calviño-Cancela and Martín-Herrero 2016, Sotille et al. 2022). The latter study brings a procedure for classification for the Hope Bay vegetation types capable to distinguish algae-, moss-, and lichen-dominated vegetation spots. In freshly green mosses, species-specific UAV-based classification based on spectral reflectance is unlikely since the spectral signatures are rather similar. However, recent study from Galindez Island (Puhovkin et al. 2022 subm.) refers to the differences caused by a vigor of a moss species caused by environmental stress. The study compares color categories of *Polytrichum strictum* and *Sanionia uncinata* (green – vigorous, brown – located under snow cover for a long time and thus loosing chlorophyll, red – typically under high cumulative PAR and drought stress). In Antarctic lichens, thanks to their contrasting spectral properties caused by their color (Barták et al. 2018) ranging from black (*e.g. Umbilicaria decussata*) to orange and yellow (*e.g. Xanthoria* sp., *Caloplaca* sp., *Candelaria* sp.), species-specific classification of lichen-dominated cover is possible. Recently, Miranda et al. (2020) were capable to distinguish *Usnea* sp. – dominated spots at the Fildes peninsula (King George Island). Similarly, Fonseca et al. (2022) distinguished spectral reflectance properties of *Usnea* sp. – dominated biological soil crust at the Harmony Point (Nelson Island, Antarctica). For the same locality, da Rosa et al. (2022) reported species-specific spectral reflectance curves and the NDVI for several moss and lichen species.

It was shown in our previous study (Váczi et al. 2020), that PRI, NDVI, GLI, RGBVI, and ExG indices (*see* Table 1) were very sensitive in the indication of moss-dominated vegetation cover. In this study, we used UAV equipped with a spectral camera to classify different elements of moss- and lichen- dominated vegetation cover in an Antarctic vegetation oasis (James Ross Island, Antarctica). We hypothesized that, apart of NDVI, other spectral indices would be sufficient tool to distinguish vegetation cover differences caused by dominating species. We also focused on the microrelief and water availability as important factors forming patchy spots of different spectral characteristics.

Material and Methods

Description of Antarctic vegetation oasis

In this work, we focused on spectral properties of vegetation cover constituents forming diverse bio-cover and mineral surfaces at a coastal terrace (63° 48′ 00″ S, 57° 52′ 56″ W, 6 m a.s.l.) of the northern part of James Ross Island. This vegetation oasis is a part of a long-term research plot (LTRP) in the neighbourhood of the Czech station (J.G.Mendel). The LTRP is located close to a coastal line in between the con-fluxes of the Bohemian and Algal streams. The area is dominated by *Bryum pseudotriquetrum* that forms carpets (Fig. 1F, 2F) in a longitudinal axis that follows the line of thawing water pathway from a temporary snowfield 50 m far from the area (Fig. 1A, 2A). In the vicinity of snow carpets are microbial mats (Fig. 1G, 2G) formed by *Nostoc* sp. colony, algae (*e.g. Zygnema* sp.) and cyanobacteria at the bottom of shallow streams vegetatively active for a short-term period during austral summer (Komárek 2013, Komárek et al. 2015). In Algal stream delta and adjacent area (Fig. 1C, 2C), a baresoil (regolith) and stone surfaces are located. In stabilized area (bankside) the stones are covered by patches of lichens, such as *e.g. Rhizoplaca melanopthalma, Xanthoria elegans* (Barták et al. 2015).

Aerial vegetation images and data processing

The long-term research plot vegetation images were acquired by using UAV Matrice 200 (DJI, Shenzhen, China) equipped with multispectral RedEdge-M camera (Micasense Inc., USA) in hight of 100 m above ground level within one flight at the stable light condition. Additionally, the reference images of calibration reflectance panel (Micasense Inc., USA) were acquired immediately before and after flight for radiometric calibration of multispectral images.

The acquired image data were processed using the structure from motion photogrammetry software Agisoft Metashape Professional *v.* 1.6 (Agisoft LLC.) to derive a multichannel orthomosaic with 4 cm spatial resolution. Spectral indices were calculated per plot from the multispectral camera's narrow-band spectral images (RedEdge-M). Several spectral indices were calculated for each image pixel and visualized in false colour scale (*see* Table 1, and Figs. 2, 3).

The images were used for the analysis of constituents of vegetation cover and characteristics of vegetation-free areas as well as the physiological status of particular bio-cover. For analysis of spectral indices at James Ross Island, the following covers were distinguished: snow field – A, tidal zone – B, water stream (Algal stream delta) – C, stony regolith – D, sand – E, moss carpets – F, soil crusts (*Nostoc* colonies dominated) – G, soil crusts wetted by meltwater – H (Fig. 1).

Values of indices for above specified areas (A – H; 130pix ≈ 0.2m^2) were determined as normalised colour value of pixels by image analysis (Image J 1.53, National Institutes of Health, Bethesda, USA).

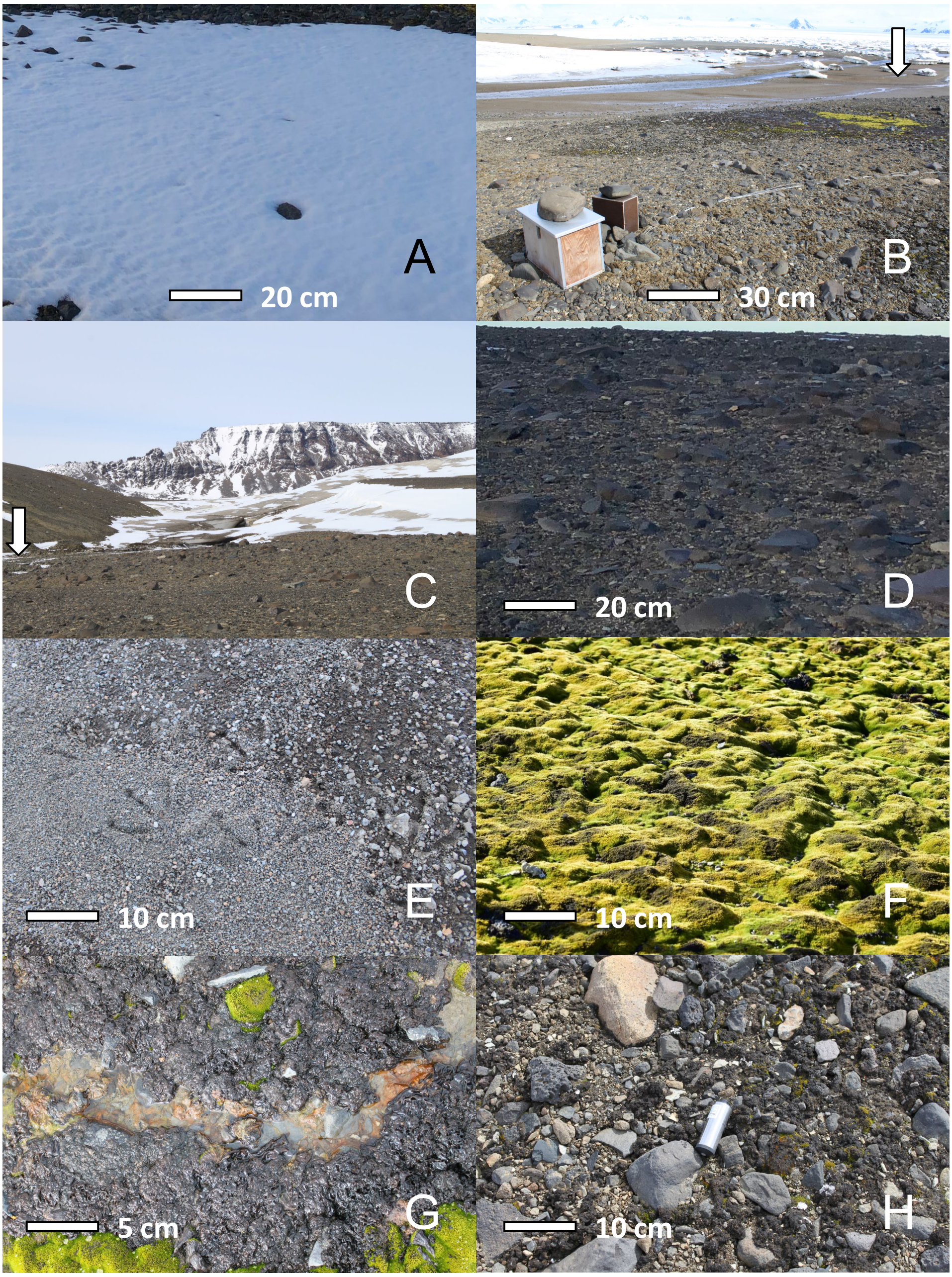

Fig. 1. Photographs of the surfaces investigated typical for the spots defined in Fig. 2 and 3: A – snow field, B – tidal zone, C – water stream (Algal stream), D – stony regolith, E – sand, F – moss carpet, G – soil crusts (*Nostoc* colonies), H – soil crusts wetted by meltwater. In the B photo, an arrow indicates a stream bottom microbiological mat. In the C photo, an arrow indicates location of the C spot in the Algal stream.

Index	Equation	Reference
Normalized Green-Red Difference Index	$NGRDI = \frac{R_G - R_R}{R_G + R_R}$	Tucker 1979
Green Leaf Index	$GLI = \frac{2 \times R_G - R_R - R_B}{2 \times R_G + R_R + R_B}$	Louhaichi et al. 2001
Triangular Greenness Index	$TGI = R_G - 0.39 \times R_R - 0.61 \times R_B$	Hunt et al. 2013
Red-Green-Blue Vegetation Index	$RGBVI = \frac{{R_G}^2 - R_R \times R_B}{{R_G}^2 + R_R \times R_B}$	Bendig et al. 2015
Normalized Excess Green Index	$ExG = \frac{2 \times R_G - R_R - R_B}{R_G + R_R + R_B}$	Woebbecke et al. 1995
Normalized Difference Vegetation Index	$NDVI = \frac{R_{NIR} - R_R}{R_{NIR} + R_R}$	Rouse et al. 1974
Red-edge Normalized Difference Vegetation Index	$NDVI_{Red-edge} = \frac{R_{NIR} - R_{RE}}{R_{NIR} + R_{RE}}$	Gitelson & Merzlyak 1994
Modified Simple Ratio Index	$MSR = \frac{R_{NIR}/R_R - 1}{\sqrt{R_{NIR}/R_R + 1}}$	Chen 1996
Red-edge Modified Simple Ratio Index	$MSR_{Red-edge} = \frac{R_{NIR}/R_{RE} - 1}{\sqrt{R_{NIR}/R_{RE} + 1}}$	Wu et al. 2008
Green Chlorophyll Index	$CI_{green} = \frac{R_{NIR}}{R_G} - 1$	Gitelson et al. 2003
Red-edge Green Chlorophyll Index	$Cl_{Red-edge} = \frac{R_{NIR}}{R_{RE}} - 1$	Gitelson et al. 2005

Table 1. Overview of applied vegetation reflectance indices calculated from narrow-band reflectance data.

Results and Discussion

This study, similarly to Jawak et al. (2019), brings data suitable for a high resolution of the components of Antarctic vegetation oases. In all studied spectral reflectance parameters, their images, respectively, snow beds were well detectable since they (with the exception of NGRDI and TGI) showed deep blue objects with well distinguishable margins (*see* spot A in the Figs. 2 and 3). Stony surfaces (D spot and majority of the area on the right side of the stream in Figs. 2 and 3) were also well distinguishable having greenish-blue color. The same was true for the coastal line formed mainly by sands and stony surfaces (*see* D spot, and the arrows showing the coastal line in Fig. 2). In VIS image as well as in the majority of spectral reflectance indices images, the stream (Algal stream, James Ross Island) forming a 2-arm delta with a complex multiple branching and junction pattern was well distinguishable, typically by blue color. In spite of the fact the freshwater of the Algal stream is typically inhabited by a relatively small biomass of microalgae and cyanobacteria in austral summer season (Kopalová et al. 2013, Skácelová et al. 2013), no indication in NDVI was apparent. The only exception was a blind arm of the Bohemian stream (see the yellow spot close to B spot in Fig. 2) – mode details below in the NDVI discussion.

Numeric values of the studied spectral reflectance images differed for the A to H spots (*see* Table 2) suggesting their great potential in vegetation mapping of ice-free areas. NDVI image showed the NDVI distribution over the long-term research plot having the highest values for the areas where moss vegetation occurred (*see* F spot) followed by a *Nostoc*-dominated seepage. This is well comparable to the field studies from polar regions that report high NDVI values for vigorous, well hydrated and physiologically active moss communities (Lucieer et al. 2012, 2014; Turner et al. 2014). High NDVI values occurred also in a close proximity to the F spot (outside of the margins of yearly melting snowfield) which represented biological soil crusts dominated by microalgae and cyanobacteria freshly exposed to light after the snow bed retreat (MB, PV – personal *in situ* observation). Distribution of these close-to-snow bed margins spots showing high NDVI corresponded well to the distribution of meltwater on the day of the UAV flight. These spots are well distinguishable also in the other spectral reflectance parameters (*see* e.g. $NDVI_{Red\text{-}edge}$, NGRDI in Figs 2, 3). The close-to B spot area showing high NDVI values (*see* yellow area in the NDVI image) might be associated with microautotrophs that are accumulated in the bottom of one arm of the Bohemian stream during low tide period. This accumulation forms a microbiological mat fixed to the stream bottom and is ´visible´ only during low tide events. This is well comparable with the results of Salvatore et al. (2020), who investigated the Crescent Stream in the Fryxell basin and found NDVI values related to the abundance of autotrops-dominated microbiological mats formed at stream bottom. Our results do not show high NDVI values along the whole stream because of generally low abundance of microautotrophs, and a high amount of mineral particles transported by the stream. However, ExG and GLI indices indicate mats distribution in the streams (*see* arrows in Figs. 2, 3). Our data from the stream bottom suggest that the technique might be used in the investigation of Antarctic aquatic environments, such as *e.g.* seepages and shallow freshwater lakes, aimed to the evaluation of spectral libraries of particular vegatation classes (*see* e.g. da Rosa et al. 2021).

Moss carpets (F spot and neighbouring patches) were well distingushable by the GLI, RGBVI, and ExG spectral indices, similarly to the previous study (Váczi et al. 2020). This is consistent with earlier experience with *e.g.* RGBVI, which is generally used for detection of freshly green vegetation (Lee et al. 2021). Similarly, ExG spectral reflectance index was used successfully for classification of moss-dominated vegetation in Iceland (Gatzouras 2015). Recently, spectral characteristics of Antarctic vegetation are in focus of many studies using an UAV-based remote sensing approach. Main emphasis is to measure spectral reflectance curves and evaluate spectral reflectance indices in order to contribute to a spectral library (Chi et al. 2021) of vegetation components in polar regions. Our study contributes by 10 different vegetation-dominated or vegetation-free surfaces. Since remote sensing of vegetation is widely used in polar research, forthcoming studies will be oriented to the spectral signatures of particular species of mosses and lichens, as well as algae- and/or cyanobacteria-dominated seepages and mats. This UAV-based approach together with ground inspection outputs can provide helpful information of Antarctic vegetation oases in difficult-to-access or distant areas.

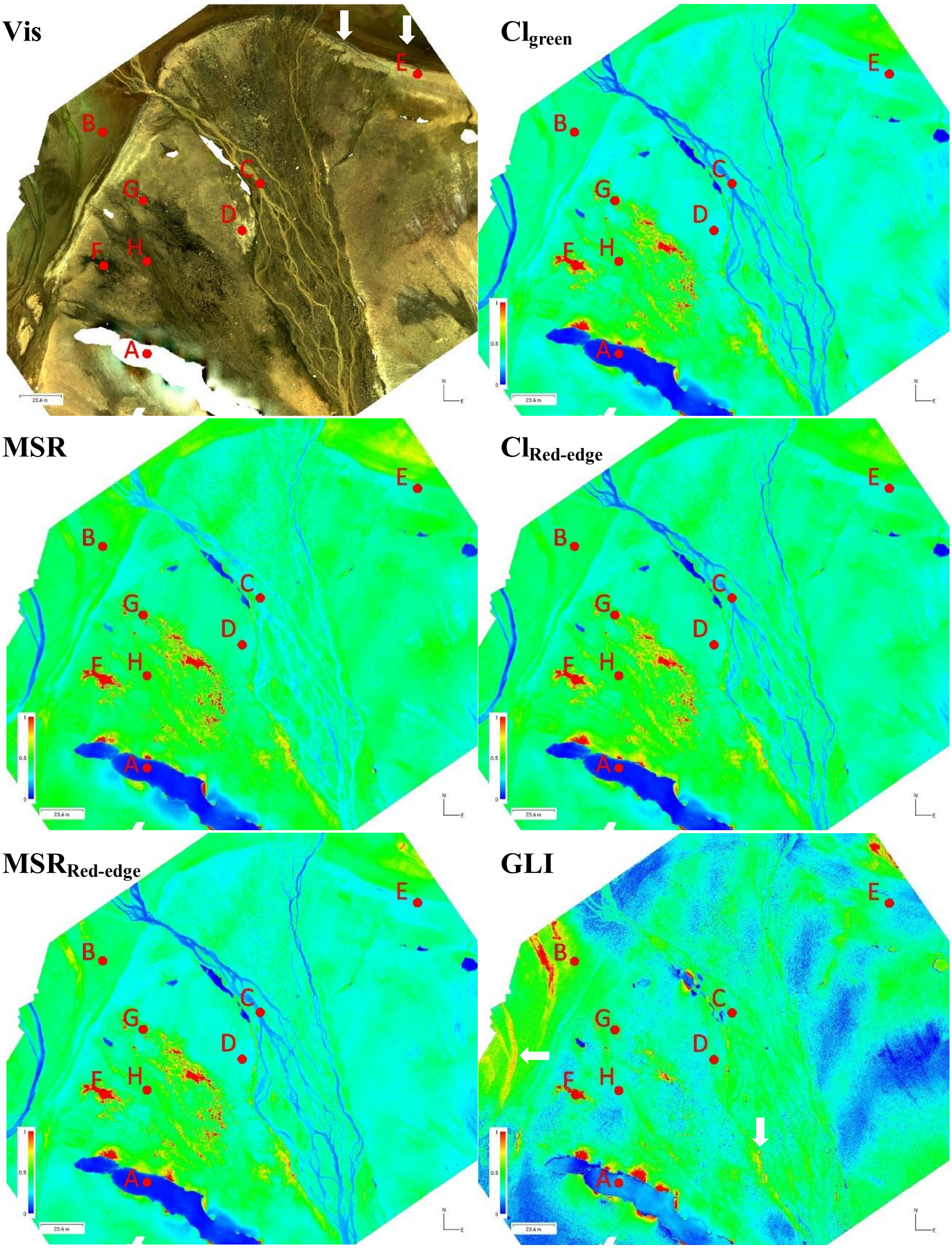

Fig. 2. Visual (VIS) and false colour images of MSR, $MSR_{Red\text{-}edge}$, Cl_{green}, $Cl_{Red\text{-}edge}$, and GLI indices distribution on long-term research plot (LTRP), James Ross Island, Antarctica with highlighted localities of different surface and vegetation types (*see* Table 2).

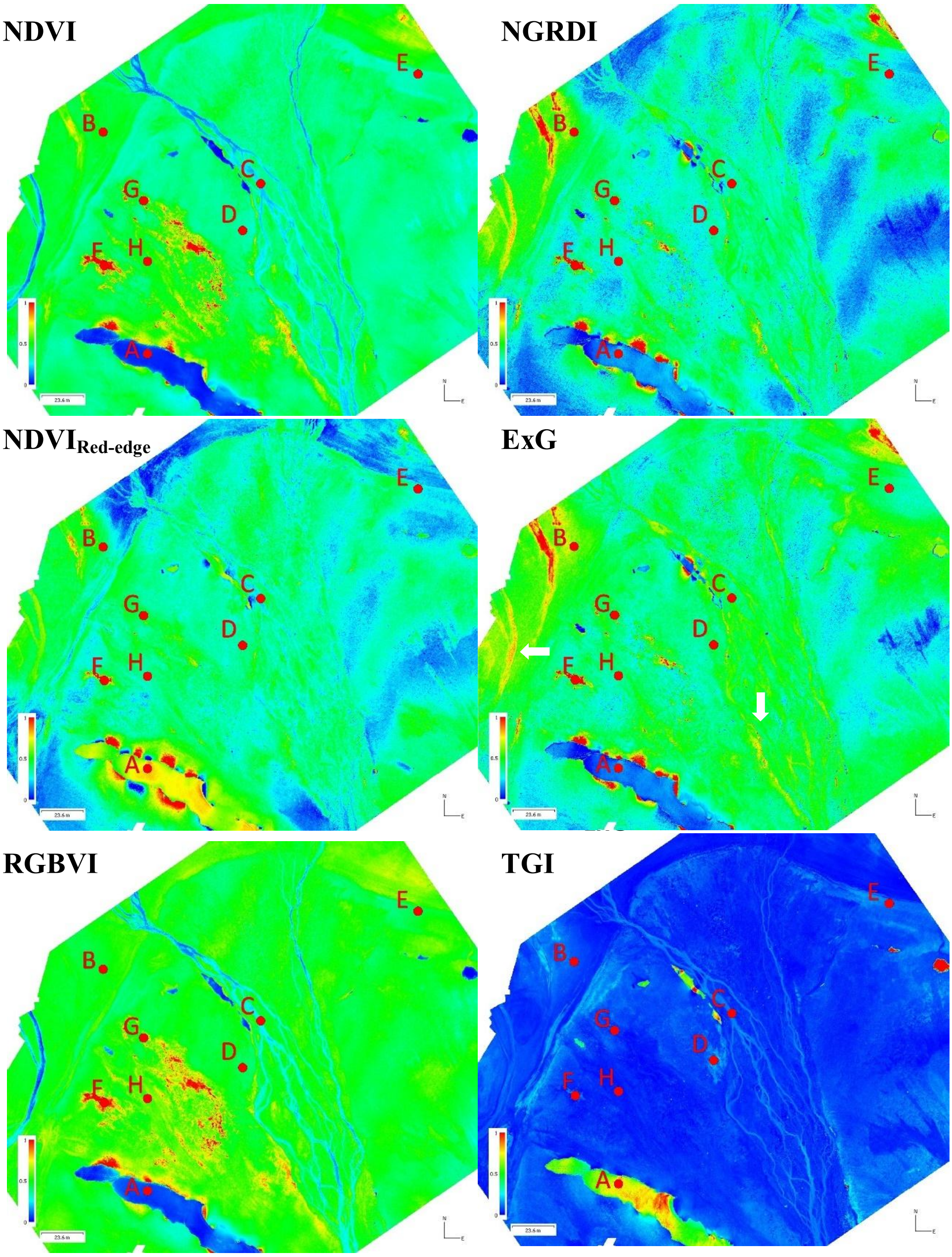

Fig. 3. False colour images of NDVI, $NDVI_{Red\text{-}edge}$, RGBVI, NGRDI, ExG, and TGI indices distribution on long-term research plot (LTRP), James Ross Island, Antarctica with highlighted localities of different surface and vegetation types (compare with Fig. 2).

area	MSR	$MSR_{Red\text{-}edge}$	CI_{green}	$CI_{Red\text{-}edge}$	GLI	NDVI	$NDVI_{Red\text{-}edge}$	RGBVI	NGRDI	ExG	TGI
A	**0.000** *0.000*	**0.093** *0.003*	**0.000** *0.000*	**0.138** *0.002*	**0.172** *0.020*	**0.106** *0.002*	**0.000** *0.000*	**0.669** *0.020*	**0.643** *0.008*	**0.134** *0.017*	**0.772** *0.040*
B	**0.600** *0.049*	**0.309** *0.012*	**0.791** *0.052*	**0.319** *0.010*	**0.674** *0.074*	**0.254** *0.007*	**0.915** *0.058*	**0.052** *0.004*	**0.454** *0.041*	**0.703** *0.057*	**0.107** *0.013*
C	**0.162** *0.036*	**0.202** *0.019*	**0.356** *0.045*	**0.225** *0.016*	**0.370** *0.038*	**0.182** *0.013*	**0.209** *0.054*	**0.043** *0.011*	**0.264** *0.045*	**0.513** *0.038*	**0.115** *0.019*
D	**0.304** *0.026*	**0.277** *0.012*	**0.460** *0.053*	**0.290** *0.011*	**0.334** *0.036*	**0.233** *0.008*	**0.441** *0.043*	**0.061** *0.009*	**0.355** *0.035*	**0.384** *0.031*	**0.133** *0.039*
E	**0.321** *0.017*	**0.291** *0.008*	**0.553** *0.038*	**0.302** *0.007*	**0.316** *0.049*	**0.242** *0.005*	**0.471** *0.031*	**0.050** *0.005*	**0.310** *0.022*	**0.397** *0.045*	**0.127** *0.013*
F	**0.996** *0.008*	**0.651** *0.051*	**1.000** *0.000*	**0.661** *0.058*	**0.927** *0.148*	**0.444** *0.025*	**1.000** *0.000*	**0.012** *0.016*	**0.732** *0.181*	**0.925** *0.147*	**0.090** *0.046*
G	**0.573** *0.046*	**0.389** *0.021*	**0.823** *0.073*	**0.391** *0.019*	**0.368** *0.055*	**0.302** *0.013*	**0.881** *0.066*	**0.064** *0.004*	**0.406** *0.028*	**0.387** *0.054*	**0.046** *0.011*
H	**0.556** *0.042*	**0.385** *0.016*	**0.926** *0.068*	**0.388** *0.016*	**0.292** *0.047*	**0.299** *0.008*	**0.855** *0.066*	**0.053** *0.003*	**0.322** *0.020*	**0.358** *0.051*	**0.030** *0.009*

Table 2. Spectral reflectance indices (mean values and standard deviations) recorded for different spots of the long-term research plot (LTRP) located in a close proximity of J.G. Mendel station (James Ross Island, Antarctica). Spot abbreviation: A – snow field, B – tidal zone, C – water stream (Algal stream delta), D – stony regolith, E – sandy surface, F – moss carpet, G – soil crust (*Nostoc* colonies dominated), H – soil crusts wetted by meltwater.

Concluding remarks

For vegetation science and mapping of Antarctic vegetation oases, spectral library of different vegetation classes and species-specific components is of great importance (*see* e.g. spectral library of the Korea Polar Data Center – Other sources). Future development of such spectral libaries will focus on single species-dominated spots, especially in lichens which have species-specific spectral signatures (Barták et al. 2018). However, definition of their spectral properties represents a critical requirement for improving vegetation remote sensing in polar regions. For mosses, due to their generally green color in vigorous state, resolution of species specifity is a challenge. However, Turner et al. (2018) suggested a combined approach for moss-dominated vegetation oasis. This approach combines spectral reflectance-based remote imaging and modelling in order to evaluate species and health status of moss cushions. Future development of advanced miniaturized sensors and image processing technologies will facilitate this trend allowing analyses of monospecific spots with area below 10 cm^2.

References

BARTÁK, M., HÁJEK, J., MORKUSOVÁ, J., SKÁCELOVÁ, K. and KOŠUTHOVÁ, A. (2018): Dehydration-induced changes in spectral reflectance indices and chlorophyll fluorescence of Antarctic lichens with different thallus color, and intrathalline photobiont. *Acta Physiologiae Plantrum*, 40: 177. doi: 10.1007/s11738-018-2751-3

BARTÁK, M., VÁCZI, P., STACHOŇ, Z. and KUBEŠOVÁ, S. (2015): Vegetation mapping of moss-dominated areas of northern part of James Ross Island (Antarctica) and a suggestion of protective measures. *Czech Polar Reports*, 5: 75-87.

BEAMISH, A., RAYNOLDS, M. K., EPSTEIN, H., FROST, G. V., MACANDER, M. J., BERGSTEDT, H., BARTSCH, A., KRUSE, S., MILES, V., TANIS, C. M., HEIM, B., FUCHS, M., CHABRILLAT, S., SHEVTSOVA, I., VERDONEN, M. and WAGNER, J. (2020): Recent trends and remaining challenges for optical remote sensing of Arctic tundra vegetation: A review and outlook. *Remote Sensing of Environment*, 246: 111872.

BENDIG, J., YU, K., AASEN, H., BOLTEN, A., BENNERTZ, S., BROSCHEIT, J., GNYP, M. L. and BARETH, G. (2015): Combining UAV-based plant height from crop surface models, visible, and near infrared vegetation indices for biomass monitoring in barley. *International Journal of Applied Earth Observation and Geoinformation*, 39: 79-87.

CALVIÑO-CANCELA, M., MARTÍN-HERRERO, J. (2016): Spectral discrimination of vegetation classes in ice-free areas of Antarctica. *Remote Sensing*, 8: 856. doi: 10.3390/rs8100856

CHEN, J. M. (1996): Evaluation of vegetation indices and a modified simple ratio for boreal applications. *Canadian Journal of Remote Sensing*, 22: 229-242. doi: 10.1080/07038992.1996.10855178

CHI, J., LEE, H., HONG, S.G. and KIM, H.-C. (2021): Spectral characteristics of the Antarctic vegetation: A case study of Barton Peninsula. *Remote Sensing*, 13(13): 2470. doi: 10.3390/rs13132470

DA ROSA, C., PEREIRA FILHO, W., BREMER, U., ANDRADE, A., KRAMER, G., HILLEBRAND, F. and JESUS, J. (2021): The limnology and spectral behaviour of a freshwater lake at Harmony Point, Nelson Island, Antarctica. *Antarctic Science*, 33(5): 479-492. doi:10.1017/S0954102021000304

DA ROSA, C. N., PEREIRA FILHO, W., BREMER, U. F., PUTZKE, J., DE ANDRADE, A. M., KRAMER, G., HILLEBRAND, F. and DE JESUS, J. B. (2022): Spectral behavior of vegetation in Harmony Point, Nelson Island, Antarctica. *Biodiversity and Conservation*, 31(7): 1-19. doi: 10.1007/s10531-022-02408-7.

EISCHEID, I., SOININEN, E. M., ASSMANN, J. J., IMS, R.A., MADSEN, J., PEDERSEN, Å. Ø., PIROTTI, F., YOCCOZ, N. G. and RAVOLAINEN, V. T. (2021): Disturbance mapping in Arctic tundra improved by a planning workflow for drone studies: Advancing tools for future ecosystem monitoring. *Remote Sensing*, 13(21): 4466. doi: 10.3390/rs13214466

FONSECA, E. L., SANTOS, E., FIGUEIREDO, A. R. and SIMÕES, J. C. (2022): Antarctic biological soil crusts surface reflectance patterns from landsat and sentinel-2 images. *Anais da Academia Brasileira de Ciencias [Annals of the Brazilian Academy of Sciences]*, 94(suppl 1): e20210596. doi: 10.1590/0001-3765202220210596

FRASER, R.H., OLTHOF, I., LANTZ, T.C. and SCHITT, C. (2016): UAV photogrammetry for mapping vegetation in the low-Arctic. *Arctic Science*, 2(3): 79-102. doi: 10.1139/as-2016-0008.

GATZOURAS, M. (2015): Assessment of trampling impact in Icelandic natural areas in experimental plots with focus on image analysis of digital photographs. Thesis, No. 351, Department of Physical Geography and Ecosystem Science, Lund University, Sweden, 45 p.

GITELSON, A. A., GRITZ, Y. and MERZLYAK, M. N. (2003): Relationships between leaf chlorophyll content and spectral reflectance and algorithms for non-destructive chlorophyll assessment in higher plant leaves. *Journal of Plant Physiology*, 160: 271-282.

GITELSON, A. A., VIÑA, A., CIGANDA, V., RUNDQUIST, D. C. and ARKEBAUER, T. J. (2005): Remote estimation of canopy chlorophyll content in crops. *Geophysical Research Letters,* 32(8): 1-4. doi: 10.1029/2005GL022688

GITELSON, A., MERZLYAK, M. N. (1994): Spectral reflectance changes associated with autumn senescence of *Aesculus hippocastanum* L. and *Acer platanoides* L. leaves. Spectral features and relation to chlorophyll estimation. *Journal of Plant* Physiology, 143: 286-292. doi: 10.1016/S0176-1617(11)81633-0

GRAY, A., KROLIKOWSKI, M., FRETWELL, P., CONVEY, P., PECK, L. S., MENDELOVA, M., SMITH, A. G. and DAVEY, M. P. (2020): Remote sensing reveals Antarctic green snow algae as important terrestrial carbon sink. *Nature Communications*, 11: 2527.

HUNT, E. R., DORAISWAMY, P. C., MCMURTREY, J. E., DAUGHTRY, C. S., PERRY, E. M. and AKHMEDOV, B. (2013): A visible band index for remote sensing leaf chlorophyll content at the canopy scale. *International Journal of Applied Earth Observation and Geoinformation*, 21: 103-112. doi: 10.1016/j.jag.2012.07.020

JAWAK, S. D., LUIS, A. J., FRETWELL, P. T., CONVEY, P. and DURAIRAJAN, U. A. (2019): Semiautomated detection and mapping of vegetation distribution in the Antarctic environment using spatial-spectral characteristics of WorldView-2 Imagery. *Remote Sensing*, 11(16): 1909. doi: 10.3390/rs11161909

KOMÁREK, J. (2013): Phenotypic and ecological diversity of freshwater coccoid cyanobacteria from maritime Antarctica and islands of NW Weddell Sea. I. Synechococcales. *Czech Polar Reports*, 3(2): 130-143.

KOMÁREK, J., GENUÁRIO, D. B., FIORE, M. F. and ELSTER, J. (2015): Heterocytous cyanobacteria of the Ulu Peninsula, James Ross Island, Antarctica. *Polar Biology*, 38: 475-492. doi: 10.1007/s00300-014-1609-4.

KOPALOVÁ, K., NEDBALOVÁ, L., NÝVLT, D., ELSTER, J. and VAN DE VIJVER, B. (2013): Diversity, ecology and biogeography of the freshwater diatom communities from Ulu Peninsula (James Ross Island, NE Antarctic Peninsula). *Polar Biology*, 36: 933-948. doi: 10.1007/s00300-013-1317-5

LEE, G., HWANG, J. and CHO, S. (2021): A novel index to detect vegetation in urban areas using uav-based multispectral images. *Applied Science*, 11: 3472. doi: 10.3390/app11083472

LEVY, J., CARY, S., JOY, K. and LEE, C. (2020): Detection and community-level identification of microbial mats in the McMurdo Dry Valleys using drone-based hyperspectral reflectance imaging. *Antarctic Science*, 32(5): 367-381. doi:10.1017/S0954102020000243

LOUHAICHI, M., BORMAN, M. M. and JOHNSON, D. E. (2001): Spatially located platform and aerial photography for documentation of grazing impacts on wheat. *Geocarto International*, 16: 65-70

LUCIEER, A., ROBINSON, S., TURNER, D., HARWIN, S. and KELCEY, J. (2012): Using a micro-UAV for ultra-high resolution multi-sensor observations of Antarctic moss beds. 15th Australasian Remote Sensing & Photogrammetry, Conference. Alice Springs. 14-16th Sept 2010. ISPRS -

International Archives of the Photogrammetry, Remote Sensing and Spatial Information Sciences. XXXIX-B1, pp. 429–433. doi: 10.5194/isprsarchives-XXXIX-B1-429-2012.

LUCIEER, A., TURNER, D., KING, D. and ROBINSON, S. (2014): Using an Unmanned Aerial Vehicle (UAV) to capture micro-topography of Antarctic moss beds. *International Journal of Applied Earth Observation and Geoinformation*, 27: 53-62. doi: 10.1016/j.jag.2013.05.011

MIRANDA, V., PINA, P., HELENO, S., VIEIRA, G., MORA, C. and SCHAEFER, C.E.G.R. (2020): Monitoring recent changes of vegetation in Fildes Peninsula (King George Island, Antarctica) through satellite imagery guided by UAV surveys. *Science of The Total Environment*, 704: 135295.

PINA, P., VIEIRA, G. (2022): UAVs for science in Antarctica. *Remote Sensing*, 14(7):1610. doi: 10.3390/rs14071610

PUHOVKIN, A., BARTÁK, M., SHEPETA, Y., DZHULAI, A., KAZANTSEV, T. and PARNIKOZA, I. (2022, subm.): Impact of environmental factors on the moss banks interannual development and their spectral/vitality parameters in the Galindez Island (Argentine Islands, West Antarctica). *Polar Science*

ROUSE, J. W., J., HAAS, R. H., SCHELL, J. A. and DEERING, D. W. (1974): Monitoring vegetation systems in the Great Plains with ERTS. *In*: NASA. Goddard Space Flight Center 3d ERTS-1 Symp., Vol. 1, Sect. A. pp. 309–317.

SALVATORE, M. R., BORGES, S. R., BARRETT, J. E., SOKOL, E. R., STANISH, L. F., POWER, S. N. and MORIN, P. (2020): Remote characterization of photosynthetic communities in the Fryxell basin of Taylor Valley, Antarctica. *Antarctic Science*, 32: 255-270.

SIEWERT, M. B, OLOFSSON, J. (2020): Scale-dependency of Arctic ecosystem properties revealed by UAV. *Environmental Research Letters*, 15: 129601

SKÁCELOVÁ, K., BARTÁK, M., COUFALÍK, P., NÝVLT, D. and TRNKOVÁ, K. (2013): Biodiversity of freshwater algae and cyanobacteria on deglaciated northern part of James Ross Island, Antarctica. A preliminary study. *Czech Polar Reports*, 3: 93-106.

SOTILLE, M. E., BREMER, U. F., VIEIRA, G., VELHO, L. F., PETSCH, C., AUGER, J. D. and SIMÕES, J. C. (2022): UAV-based classification of maritime Antarctic vegetation types using GEOBIA and random forest. *Ecological Informatics*, 71: 101768. doi: 10.1016/j.ecoinf.2022.101768

TUCKER, C. J. (1979): Red and photographic infrared linear combinations for monitoring vegetation. *Remote Sensing of Environment*, 8: 127-150.

TURNER, D., LUCIEER, A., MALENOVSKÝ, Z., KING, D. and ROBINSON, S. (2014): Spatial co-registration of ultra-high resolution visible, multispectral and thermal images acquired with a micro-UAV over Antarctic moss beds. *Remote Sensing,* 6(5): 4003-4024. doi: 10.3390/rs6054003

TURNER, D., LUCIEER, A., MALENOVSKÝ, Z., KING, D. and Robinson, S.A. (2018): Assessment of Antarctic moss health from multi-sensor UAS imagery with Random Forest Modelling. *International Journal of Applied Earth Observation and Geoinformation*, 68: 168-179.

VÁCZI. P., BARTÁK, M., BEDNAŘÍKOVÁ, M., HRBÁČEK, F. and HÁJEK, J. (2020): Spectral properties of Antarctic and Alpine vegetation monitored by multispectral camera: Case studies from James Ross Island and Jeseníky Mts. *Czech Polar Reports*, 10(2): 297-312.

WOEBBECKE, D. M., MEYER, G. E., VON BARGEN, K. and MORTENSEN, D. A. (1995): Color indices for weed identification under various soil, residue, and lighting conditions. *Transactions of the ASAE*, 38: 259-269.

WU, C., NIU, Z., TANG, Q. and HUANG, W. (2008): Estimating chlorophyll content from hyperspectral vegetation indices: Modeling and validation. *Agric For Meteorol*, 148: 1230-1241. doi: 10.1016/J.AGRFORMET.2008.03.005

Web sources / Other sources

Korea Polar Data Center (https://kpdc.kopri.re.kr)